

Orbitally Dependent Exchange in Two Sulfur-Bridged Binuclear Iron(II) Complexes. Magnetic Exchange in Transition Metal Complexes. 11¹

A. P. Ginsberg,^{*2a} M. E. Lines,^{*2a} K. D. Karlin,^{2b} S. J. Lippard,^{*2b}
and F. J. DiSalvo^{2a}

Contribution from Bell Laboratories, Murray Hill, New Jersey 07974, and the
Department of Chemistry, Columbia University, New York, New York 10027.
Received January 26, 1976

Abstract: Orbitally dependent exchange is defined as exchange in a cluster with one or more orbital states thermally accessible from an orbital singlet ground state. A theory based on the hypothesis of orbitally dependent exchange is shown to account quantitatively, in a physically understandable manner, for the susceptibility vs. temperature curves of the five-coordinate di- μ -thiolato-bridged Fe(II) dimers (FeL)₂ and (FeL')₂, where LH₂ is *N,N'*-dimethyl-*N,N'*-bis(2-mercaptoethyl)ethylenediamine and L'H₂ is *N,N'*-dimethyl-*N,N'*-bis(2-mercaptoethyl)-1,3-propanediamine. Because the exchange in these complexes is orbitally dependent it is possible to evaluate the electron pair exchange parameters, contributing to the net exchange between iron atoms, from the temperature dependence of the susceptibility. The pair parameters obtained in this manner indicate that two Fe²⁺ atoms 3.21 Å apart can engage in significant antiferromagnetic exchange ($|J| \sim 50 \text{ cm}^{-1}$) by direct overlap of 3d orbitals pointed along the iron-iron internuclear line. This direct exchange is extremely sensitive to distance, and an increase of 0.16 Å in $d(\text{Fe} \cdots \text{Fe})$ causes a decrease of at least $\sim 50\%$ in the exchange parameter.

Exchange coupling in cluster complexes has been extensively studied for the case of metal atoms in single-ion orbital singlet ground states. It is normally found that the exchange split cluster energy levels are given by the isotropic spin-coupling Hamiltonian

$$\mathcal{H} = -2 \sum_{\text{atom pairs } i,j} J_{ij} \mathbf{S}_i \cdot \mathbf{S}_j \quad (1)$$

where J_{ij} is the exchange parameter for the intracluster interaction between metal atoms i and j with spin operators \mathbf{S}_i and \mathbf{S}_j . Comparison of experimental susceptibility vs. temperature measurements with the susceptibility equation derived from eq 1 generally enables the J_{ij} to be evaluated. If, as is often the case, however, J_{ij} is the resultant of two or more electron-pair exchanges, the susceptibility-temperature curve does not ordinarily provide sufficient information to allow the components of J_{ij} to be determined. The present paper describes an unusual situation in which analysis of the temperature dependence of the susceptibility of two Fe(II) dimers has led to the semiquantitative determination of three electron-pair exchange integrals contributing to the net intradimer exchange. This determination is possible because, although the single-ion ground state is orbitally nondegenerate, there is a second low energy orbital state not far removed from the ground state. As a consequence there are four orbital dimer energy levels, two of which are degenerate, within which exchange coupling occurs over the temperature range studied. Each orbital dimer state is characterized by a different exchange parameter, so that the temperature dependence of the susceptibility is determined by three exchange parameters. Since each of these parameters is a function of the same three electron-pair exchange integrals, there are three relations between the orbital dimer state exchange parameters and the electron-pair exchange integrals. The latter may therefore be evaluated from the temperature dependence of the susceptibility.

We use the term "orbitally dependent exchange" to refer to exchange in a cluster with one or more orbital states thermally accessible from an orbital singlet ground state. We believe that orbitally dependent exchange occurs in the complexes (FeL)₂ and (FeL')₂, where LH₂ is *N,N'*-dimethyl-*N,N'*-bis(2-mercaptoethyl)ethylenediamine and L'H₂ is *N,N'*-dimethyl-*N,N'*-bis(2-mercaptoethyl)-1,3-propanediamine. Both molecules are di- μ -thiolato-bridged iron dimers; Figure 1 shows

their molecular structures.³ The primed and unprimed atoms are related by a center of symmetry, and the bridging atoms Fe, S1, Fe', S1' are coplanar. The coordination geometry about each iron atom in (FeL')₂ is best described as a slightly distorted trigonal bipyramid with atoms N1, S2, and S1' forming an equatorial plane. (FeL)₂ has a similar structure except that instead of three there are now only two methylene groups between the two donor nitrogen atoms. All bonded iron-sulfur and iron-nitrogen distances are comparable in (FeL')₂ and (FeL)₂. However, as shown by the change in the S1-Fe-N2 angle from 172° in (FeL')₂ to 158° in (FeL)₂ and of the N1-Fe-N2 angle from 90° in (FeL')₂ to 79° in (FeL)₂, the latter is much more distorted from regular trigonal bipyramidal geometry. Differences in the nonbonded iron-iron distance and the angle at the bridging sulfur atom for the two complexes (Figure 1) are of critical importance in understanding the exchange coupling. In particular, it should be noted that $d(\text{Fe} \cdots \text{Fe}')$ is 0.16 Å shorter in (FeL)₂ than in (FeL')₂ while angle Fe-S1-Fe' has a greater deviation from 90° in the former than in the latter compound.

Measurements in the temperature range 4.2-370 K give susceptibility vs. temperature curves which have a broad maximum at ~ 170 K for (FeL')₂ and a maximum or plateau at ~ 370 K for (FeL)₂. We show that these curves cannot be accounted for on the assumption of exchange between isolated orbital singlet ground states. The experimental results are, however, very well accounted for by the orbitally dependent exchange theory. This model leads to the interesting conclusion that in (FeL)₂ the antiferromagnetic coupling is predominantly due to direct overlap of 3d-orbitals directed along the iron-iron internuclear direction. The direct exchange is much smaller in (FeL')₂, consistent with the longer Fe \cdots Fe distance in this compound.

Experimental Section

(FeL')₂ and (FeL)₂ were prepared and characterized at Columbia University, as described in the preceding paper.⁴ Samples for magnetic susceptibility measurements were delivered to Bell Laboratories in nitrogen-filled Schlenk flasks. Subsequent handling was in an Argon filled glove box equipped with a Vacuum Atmospheres Corp. recirculating system. Samples were loaded into quartz tubes and sealed off under helium. Susceptibility measurements were carried out with an electronic Faraday balance over the range 4.3-372 K at 4.3 kOe. Field dependence was checked at 4.3 and 298 K by varying the field

from 1 to 13 kOe. The equipment was calibrated as described previously.⁵

Results

Table I contains the results of our measurements in the form of χ_A' , the field independent susceptibility per gram-atom of iron. A diamagnetic correction has been included in the susceptibilities.⁶ Plots of χ_A' vs. T may be seen in Figures 4–7. The susceptibility of $(\text{FeL}')_2$ passes through a maximum at ~ 170 K and then falls to a minimum at ~ 7 K. $(\text{FeL})_2$ behaves similarly, except that the maximum is shifted to higher temperature and appears only as a plateau; the minimum occurs at ~ 16 K and the low temperature susceptibility rise is much greater than in $(\text{FeL}')_2$. Susceptibility curves with high temperature maxima and low temperature minima are frequently encountered and are typical of antiferromagnetically coupled clusters with small amounts of paramagnetic impurity.^{7a} Confirmation that the low temperature rise in the susceptibility of $(\text{FeL}')_2$ and $(\text{FeL})_2$ is due to an impurity is provided by magnetic Mossbauer measurements,⁴ which show that the dimers have no free spin at 4.3 K. Knowing this, we obtained a correction for the paramagnetic impurity as follows: At 4.3 K the measured susceptibility is the sum of the Curie susceptibility of the impurity and the temperature independent paramagnetism of the dimer. The line obtained by plotting the measured susceptibility values at temperatures below the minima against $1/T$ has an intercept that gives the dimer TIP, and a slope determined by the impurity Curie susceptibility. $(\text{FeL}')_2$ has a TIP of $530 \times 10^{-6} \text{ cm}^3 \text{ g-atom}^{-1}$ and its impurity susceptibility per 0.5 mol of dimer is given by $\chi_{\text{impurity}} = 1.82 \times 10^{-3}/T \text{ cm}^3 \text{ g-atom}^{-1}$. For $(\text{FeL})_2$, the TIP is $615 \times 10^{-6} \text{ cm}^3 \text{ g-atom}^{-1}$ and $\chi_{\text{impurity}} = 4.59 \times 10^{-3}/T \text{ cm}^3 \text{ g-atom}^{-1}$. The impurity susceptibility would be accounted for by $\leq 0.1\%$ of Fe(II) impurity with $\mu_{\text{eff}} = 5.4 \mu_B$. The corrected susceptibilities $\chi_A'(\text{corr}) = \chi_A' - \chi_{\text{impurity}}$ are given in Table I and in Figures 4–7. Also in Table I are the values of $\mu_{\text{eff}} = 2.8273(\chi_A'(\text{corr})T)^{1/2}$.

Crystal Field Theory for the Iron Single-Ions

The ground state of a high spin free ferrous ion (Fe^{2+} , $3d^6$) is 5D with total orbital angular momentum $L = 2$ and spin $S = 2$. Since intraion exchange (i.e., Hund's rule energy) compels the first five d-electrons to enter one each the five d-orbitals $|M\rangle$ (where M can take values from -2 to $+2$ and is the quantum number of the z -component of orbital angular momentum) we can write a one to one correspondence between the many electron orbital wave functions $|d^6, M\rangle$ and the single electron orbitals $|M\rangle$ in the form

$$|d^6, M\rangle = |2\rangle|1\rangle|0\rangle|-1\rangle|-2\rangle|M\rangle \quad (2)$$

and thereby associate all the orbital moment characteristics with the single electron wave function of the sixth d electron alone. With this understanding we shall label the fivefold degenerate orbital state of the ferrous free ion by the wave function $|M\rangle$ for orbital moment calculations.

If we neglect for the moment the difference between equatorial plane S and N atoms and between bridging and non-bridging S atoms, the local environment of both Fe^{2+} ions in the idealized dimer configuration of Figure 2 is C_{3v} with the ligand atoms forming a regular trigonal bipyramid.^{7b} Taking the C_{3v} axis as the z axis, and an equatorial ligand direction as the x axis (so that the xz plane is a reflection symmetry plane), the local crystal field potential can be written in the form

$$V(r) = \sum_{n=0}^4 \sum_{m=-n}^n A_{nm} r^n Y_{nm}(\theta, \varphi) \quad (3)$$

where (r, θ, φ) are spherical polar coordinates and Y_{nm} are

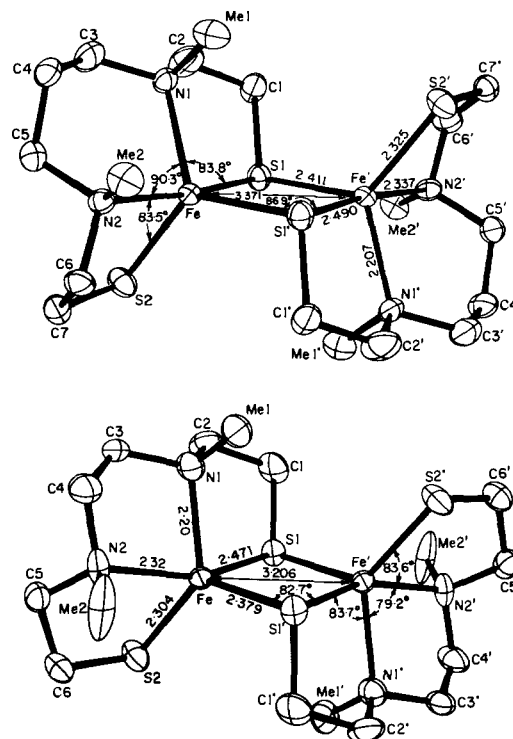


Figure 1. Molecular structure of (top) $(\text{FeL}')_2$ and (bottom) $(\text{FeL})_2$.³

spherical harmonics, with A_{nm} restricted by the C_{3v} symmetry to have nonzero values only when $m = 0, \pm 3$.⁸ Potential terms with $m = 0$ have angular momentum equivalents involving L_z alone and are therefore diagonal in the representation $|M\rangle$. However, potential terms with $m = \pm 3$ have angular momentum equivalents involving $(L^\pm)^3$ and hence give rise to matrix elements connecting $|\pm 2\rangle$ and $|\mp 1\rangle$. It follows that the orbital eigenstates of the ferrous ion in C_{3v} local environment are

$$\begin{aligned} |0'\rangle &= |0\rangle \\ |\pm 1'\rangle &= \eta[|\pm 1\rangle \pm \gamma|\mp 2\rangle] \\ |\pm 2'\rangle &= \eta[|\pm 2\rangle \pm \gamma|\mp 1\rangle] \end{aligned} \quad (4)$$

where γ is a real number with $\gamma^2 \leq 1$ and normalization parameter $\eta = (1 + \gamma^2)^{-1/2}$. In fact the character table for symmetry group C_{3v} shows that the fivefold degenerate $|M\rangle$ levels of the free ion are split into a singlet A_1 (which we now identify with $|0\rangle$) and two doublet E levels ($|\pm 1'\rangle$ and $|\pm 2'\rangle$) by a C_{3v} crystal field.

The two iron sites within the dimer do not have an identical local environment, however, even in the idealized high symmetry model. They differ in fact by an inversion symmetry. The inversion operator I transforms d orbitals $|M\rangle$ according to

$$I|M\rangle = (-1)^M|M\rangle \quad (5)$$

From eq 4 we verify that the two sets of local orbitals differ therefore only in the sign of γ .

From simple qualitative electrostatic energy considerations it is apparent that the lowest energy orbital state will be an E doublet. We expect it to be $|\pm 1'\rangle$ since this wave function contains most d_{xz} , d_{yz} character and, of the five d orbitals in the trigonal bipyramidal ligand field, the latter are almost certainly of lowest energy. However, since one can formally rewrite $|\pm 2'\rangle$ in the form

$$|\pm 2'\rangle = \eta'[|\pm 1\rangle \pm \gamma'|\mp 2\rangle] \quad (6)$$

with $\gamma' = -1/\gamma$ and $\eta'^2 = 1/(1 + \gamma'^2)$, it is not necessary to commit ourselves at this juncture and we can write the ground

Table I. Experimental Values of the Field-Independent Susceptibility per Fe Atom ($\text{cm}^3 \text{g-atom}^{-1}$) and of $\mu_{\text{eff}} (\mu_{\text{B}}) = 2.8273 (x_{\text{A}}'(\text{corr})T)^{1/2}$

	(FeL') ₂													
<i>T</i> , K	4.3	6.0	7.1	8.1	8.6	10.1	12.9	16.7	18.4	19.9	24.7	28.2	30.7	35.8
$10^5 x_{\text{A}}'^a$	95.4	83.5	79.8	79.6	79.2	85.2	113	181	216	247	344	400	430	484
$10^5 x_{\text{A}}'(\text{corr})^b$	50.6	51.5	52.7	55.8	56.9	66.2	98.1	170	205	238	336	393	424	479
μ_{eff}	0.13	0.16	0.17	0.19	0.20	0.23	0.32	0.48	0.55	0.61	0.81	0.94	1.02	1.17
<i>T</i> , K	120.1	128.4	135.6	143.7	150.7	155.7	162.3	165.1	170.8	174.9	180.7	190.4	198.0	205.3
$10^5 x_{\text{A}}'^a$	767	777	785	790	794	797	798	799	800	799	799	796	794	790
$10^5 x_{\text{A}}'(\text{corr})^b$	765	776	783	789	793	796	797	798	799	798	798	795	793	789
μ_{eff}	2.71	2.82	2.91	3.01	3.09	3.15	3.22	3.24	3.30	3.34	3.39	3.48	3.54	3.60
	(FeL) ₂													
<i>T</i> , K	4.3	8.2	10.2	14.1	15.8	18.8	20.1	22.8	25.4	27.3	30.5	35.7	40.9	45.8
$10^5 x_{\text{A}}'^c$	168	118	105	98.6	97.2	99.6	101	110	123	133	152	187	218	246
$10^5 x_{\text{A}}'(\text{corr})^b$	61.0	62.2	60.4	66.1	68.2	75.2	78.6	90.0	105	116	137	174	207	236
μ_{eff}	0.14	0.20	0.22	0.27	0.29	0.34	0.36	0.40	0.46	0.50	0.58	0.70	0.82	0.93
<i>T</i> , K	160.6	170.3	180.0	190.9	200.1	210.6	222.1	231.0	240.4	249.9	255.6	261.8	270.4	278.7
$10^5 x_{\text{A}}'^c$	444	452	459	467	473	479	485	488	492	497	500	502	505	506
$10^5 x_{\text{A}}'(\text{corr})^b$	441	450	456	464	471	477	483	486	490	495	498	500	503	505
μ_{eff}	2.38	2.47	2.56	2.66	2.74	2.83	2.93	3.00	3.07	3.14	3.19	3.23	3.30	3.35

^aDiamagnetic correction $-166 \times 10^{-6} \text{ cm}^3 \text{g-atom}^{-1}$. ^bCorrected for paramagnetic impurity as described in the text. ^cDiamagnetic correc-

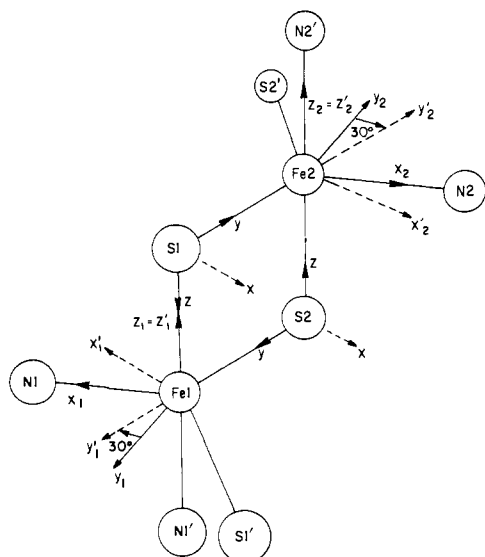


Figure 2. Idealized drawing of the local Fe^{2+} coordination in $(\text{FeL}')_2$ and $(\text{FeL})_2$. Coordinate systems used in the calculations are shown. The numbering of the atoms in this figure is not the same as in Figure 1.

doublet as

$$|\pm g\rangle = \eta[|\pm 1\rangle \pm \gamma|\mp 2\rangle] \quad (7)$$

where γ is formally an unrestricted real number. Physically we expect to find $\gamma < 1$ so that $|\pm 1\rangle$ will be the ground doublet.

The orbital degeneracy of the E-symmetry doublets is lifted in the actual dimer model of Figure 2 by the inequivalence of the equatorial ligands. In particular, if we continue to assume that the bridging and nonbridging sulfur atoms are equivalent in regard to their crystal field effects, each Fe-ligand group, with one nitrogen and two sulfur equatorial ligands, now possesses only a single symmetry element—an xz -reflection plane if the x axis is chosen to be the equatorial Fe-N direction as in Figure 2. Quite generally, by symmetry, the perturbed eigenstates must therefore be either even or odd with respect to reflection in the xz plane. Noting, from the definition of d orbitals

$$\begin{aligned} |0\rangle &= d_{z^2} \\ |\pm 1\rangle &= 2^{-1/2}[\mp d_{xz} - i d_{yz}] \\ |\pm 2\rangle &= 2^{-1/2}[d_{x^2-y^2} \pm i d_{xy}] \end{aligned} \quad (8)$$

that the E doublets are spanned by the real functions

$$\begin{aligned} \varphi_+ &= \eta[d_{yz} + \gamma d_{xy}] \\ \varphi_- &= \eta[d_{xz} - \gamma d_{x^2-y^2}] \end{aligned} \quad (9)$$

and that these functions are respectively odd and even under reflection in the xz plane, it follows that the perturbed eigenfunctions can be written in the form (eq 9) provided that the x axis is chosen to be the Fe-N direction. We shall label the energy splitting of the two lowest levels (eq 9) as Δ with φ_+ lowest if Δ is positive and assume that the other perturbed levels are sufficiently higher in energy to be neglected in further calculations (except perhaps for their contributions to g factors).

Rewriting the eigenfunctions (eq 9) in the form

$$\begin{aligned} \varphi_+ &= 2^{-1/2}\eta\{|1\rangle + |-1\rangle - \gamma\{|2\rangle - |-2\rangle\}\} \\ \varphi_- &= 2^{-1/2}\eta\{|1\rangle - |-1\rangle + \gamma\{|2\rangle + |-2\rangle\}\} \end{aligned} \quad (10)$$

one readily evaluates the matrix elements of orbital angular momentum L within φ_{\pm} . There is only one nonzero element namely

$$\langle \varphi_+ | L_z | \varphi_- \rangle = \langle \varphi_- | L_z | \varphi_+ \rangle = A \quad (11)$$

where $A = \eta^2(1 - 2\gamma^2) = (1 - 2\gamma^2)/(1 + \gamma^2)$. Given this fact it is straightforward to deduce the effect of spin-orbit coupling $\lambda L \cdot S$ on the levels $|\varphi_{\pm}, M'\rangle$, where we now recognize the five-fold spin degeneracy M' of each orbital singlet. We find that the two fivefold spin degenerate orbital levels split into four doublets (Figure 3) with energies $E = \pm(\frac{1}{4}\Delta^2 + 4A^2\lambda^2)^{1/2}$, $E = \pm(\frac{1}{4}\Delta^2 + A^2\lambda^2)^{1/2}$, and two singlets with $E = \pm\frac{1}{2}\Delta$. If $|A\lambda| \ll |\Delta|$, we see by expanding the square roots that these levels are just those produced by an effective spin perturbation DS_z^2 where $D = \pm A^2\lambda^2/\Delta$ for orbitals φ_{\mp} , respectively.

Before considering the exchange problem it is useful to get some feel for the magnitude of the parameters involved. Physically we expect γ to be ≤ 1 which implies $A \leq 1$. The only example of a γ determination for trigonal bipyramidal coordination known to us is that of Lines et al.⁹ for a Cu cation with oxygen and chlorine ligands. They find values $\gamma \approx 0.65$ -0.7 which correspond to $A \ll 1$. The spin-orbit coupling constant λ for coordinated Fe^{2+} is estimated to be $\approx -80 \text{ cm}^{-1}$ from which we conclude that $0 < |A\lambda| \leq 80 \text{ cm}^{-1}$. The magnitude of Δ at the outset is almost completely unknown. We have found no comparable information in the literature and therefore presume that Δ might be anything between a few tens and a few thousand wavenumbers.

The Exchange Hamiltonian

Isolated Orbital Singlet Ground State. For a theory of magnetic properties to be based on the lowest orbital state (φ_-

																(FeL') ₂	
40.4	45.5	50.8	55.6	60.6	65.4	71.9	75.6	79.5	84.0	90.8	94.4	100.6	104.2	110.2	116.5		
520	551	583	605	625	642	662	671	684	695	711	719	732	739	750	761		
516	547	579	601	622	639	660	669	681	692	709	717	730	737	749	759		
1.29	1.41	1.53	1.63	1.73	1.83	1.95	2.01	2.08	2.16	2.27	2.33	2.42	2.48	2.57	2.66		
220.5	231.5	240.5	250.7	260.7	270.5	278.8	290.0	300.7	309.5	321.7	330.9	340.2	350.1	360.2	365.6		
782	774	767	758	749	741	733	722	711	703	691	682	674	664	655	650		
781	773	766	758	748	740	732	721	710	702	690	682	673	664	654	649		
3.71	3.78	3.84	3.90	3.95	4.00	4.04	4.09	4.13	4.17	4.21	4.25	4.28	4.31	4.34	4.36		
																(FeL) ₂	
50.0	53.3	60.6	66.7	71.4	81.2	84.5	89.5	94.6	101.7	105.0	110.1	120.5	129.6	139.4	151.0		
267	280	307	325	336	355	361	369	376	385	389	396	407	417	425	436		
258	271	299	318	329	349	355	364	371	381	385	392	404	414	422	433		
1.01	1.08	1.20	1.30	1.37	1.50	1.55	1.61	1.68	1.76	1.80	1.86	1.97	2.07	2.17	2.29		
290.5	295.1	303.0	306.9	309.7	314.6	324.3	330.3	335.1	340.3	345.5	350.5	355.3	362.6	368.1	372.0		
509	510	512	512	511	512	512	513	513	513	514	512	513	512	512	512		
508	509	511	510	510	511	511	511	512	512	513	511	511	511	511	511		
3.43	3.46	3.52	3.54	3.55	3.58	3.64	3.67	3.70	3.73	3.76	3.78	3.81	3.85	3.88	3.90		

tion $-154 \times 10^{-6} \text{ cm}^3 \text{ g-atom}^{-1}$

or φ_+) alone it would be necessary for the upper state (φ_+ or φ_- , respectively) to escape significant thermal population to room temperature. A reasonable bound for this condition might be $\Delta > 500 \text{ cm}^{-1}$ which would lead to $|D| \lesssim 13 \text{ cm}^{-1}$. Thus, a theory justifiably neglecting the effects of all upper orbital states would have an isotropic exchange interaction $-2J\mathbf{S}_1 \cdot \mathbf{S}_2$ within the dimer (nondegenerate exchange) and a spin-orbitally induced anisotropy $-D(S_{1z}^2 + S_{2z}^2)$ with $|D| \lesssim 13 \text{ cm}^{-1}$. Since Ginsberg et al.¹⁰ have established that for $|D|$ of this order a DS_z^2 type anisotropy in an antiferromagnetic dimer context has an almost imperceptible effect on powder susceptibility to very low temperature, we shall neglect the spin-orbit splittings. Expressing the exchange Hamiltonian $-2J\mathbf{S}_1 \cdot \mathbf{S}_2$ in terms of the total spin $\mathbf{S}' = \mathbf{S}_1 + \mathbf{S}_2$ we find exchange split energy levels

$$E_0 = J[12 - S'(S' + 1)] \quad (12)$$

where $S' = 4, 3, 2, 1, 0$, and each level with spin S' is $(2S' + 1)$ -fold degenerate, in the absence of an applied field, corresponding to the z -component quantum number $M = -S', \dots, +S'$.

Orbitally Dependent Exchange. We now consider the case in which $|\Delta|$ is sufficiently small, say $0 < |\Delta| < 500 \text{ cm}^{-1}$, that both φ_+ and φ_- are thermally populated at room temperature. Since for our case $|D| = A^2\lambda^2/|\Delta|$ may well be small enough to be neglected in calculating powder susceptibility even when $|\Delta| < 500 \text{ cm}^{-1}$ we shall construct a theory which neglects the spin-orbit splittings and justify it a posteriori by finding $|D| \approx 7 \text{ cm}^{-1}$. This results in a very considerable simplification of the mathematics and allows us to proceed analytically right through to the magnetic susceptibility itself.

Our model consists of two interacting ferrous ions at sites 1 and 2 of Figure 2, each possessing two low energy orbital levels φ_{\pm} separated by an energy gap Δ . These orbital wave functions differ at sites 1 and 2 only in the sign of the parameter γ . We write then accordingly

$$\begin{aligned} \varphi_+^{(1)} &= \eta(d_{yz}^{(1)} + \gamma d_{xy}^{(1)}) \\ \varphi_-^{(1)} &= \eta(d_{xz}^{(1)} - \gamma d_{x^2-y^2}^{(1)}) \\ \varphi_+^{(2)} &= \eta(d_{yz}^{(2)} - \gamma d_{xy}^{(2)}) \\ \varphi_-^{(2)} &= \eta(d_{xz}^{(2)} + \gamma d_{x^2-y^2}^{(2)}) \end{aligned} \quad (13)$$

where the $d^{(1)}$ and $d^{(2)}$ functions are respectively the real d orbitals at sites 1 and 2 occupied by the sixth electron. The full many electron orbital wave functions can now be expressed as

$$|d^6, \varphi_{\pm}^{(i)}\rangle = |0^{(i)}\rangle |\psi_+^{(i)}\rangle |\psi_-^{(i)}\rangle |\varphi_+^{(i)}\rangle |\varphi_-^{(i)}\rangle |\varphi_{\pm}^{(i)}\rangle \quad (14)$$

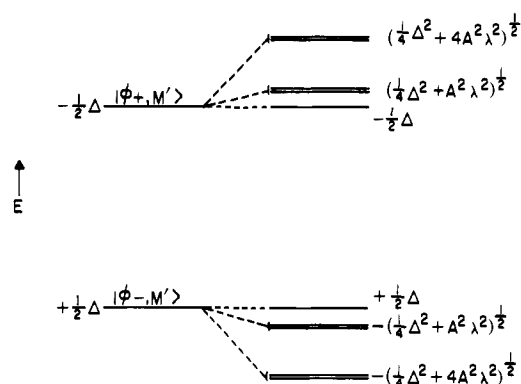


Figure 3. Single-ion orbital state energy diagram for Fe^{2+} in the dimer model. (a) The two lowest orbital states $|\varphi_{\pm}, M'\rangle$ in the absence of spin-orbit coupling and on the assumption that Δ is negative. (b) Spin-orbit splitting of the fivefold spin degenerate orbital states.

where $i = 1, 2$ and where the functions $|0\rangle = d_{z^2}$, ψ_{\pm} , and φ_{\pm} make up a complete orthogonal set, i.e.,

$$\begin{aligned} \psi_+^{(1)} &= \eta(d_{x^2-y^2}^{(1)} + \gamma d_{xz}^{(1)}) \\ \psi_-^{(1)} &= \eta(d_{xy}^{(1)} - \gamma d_{yz}^{(1)}) \\ \psi_+^{(2)} &= \eta(d_{x^2-y^2}^{(2)} - \gamma d_{xz}^{(2)}) \\ \psi_-^{(2)} &= \eta(d_{xy}^{(2)} + \gamma d_{yz}^{(2)}) \end{aligned} \quad (15)$$

Although all orbital angular momentum arises solely from the sixth electron (since the first five fill an orbital shell) the exchange arises from the singly occupied orbitals (four of them) and hence requires a knowledge of the nature of these orbitals. In particular, which four orbitals are singly occupied depends on the orbital φ_{\pm} occupied by the sixth electron.

In the absence of exchange we have four orbital dimer energy levels, viz., $|d^6, \varphi_-^{(1)}\rangle |d^6, \varphi_-^{(2)}\rangle$ with energy 2Δ , $|d^6, \varphi_+^{(1)}\rangle |d^6, \varphi_-^{(2)}\rangle$ and $|d^6, \varphi_-^{(1)}\rangle |d^6, \varphi_+^{(2)}\rangle$ both with energy Δ , and $|d^6, \varphi_+^{(1)}\rangle |d^6, \varphi_+^{(2)}\rangle$ with energy zero. Each of these levels is 25-fold spin degenerate by virtue of the fivefold spin degeneracy ($S = 2$) of each single ion orbitally nondegenerate level. Thus each dimer level is split into 25 spin levels by an exchange perturbation $-2J\mathbf{S}_1 \cdot \mathbf{S}_2$. The exchange will be isotropic because each single-ion level involved is orbitally nondegenerate. However, as pointed out above, the value of the exchange parameter J will *not* be the same for each orbital dimer level but will depend on the character of the singly occupied orbitals in each case. We write accordingly three different exchange parameters: J_{++} (when the two φ_+ orbitals are singly occupied, i.e., the sixth electrons are in φ_- orbitals),

$J_{+-} = J_{-+}$ (when one φ_+ and one φ_- is singly occupied) and finally J_{--} (when both φ_- orbitals are singly occupied). The exchange splitting within each orbital dimer level will have the same form as eq 12, and we write

$$\begin{aligned} E_{++} &= 2\Delta + J_{++}[12 - S'(S' + 1)] \\ E_{+-} &= E_{-+} = \Delta + J_{+-}[12 - S'(S' + 1)] \\ E_{--} &= J_{--}[12 - S'(S' + 1)] \end{aligned} \quad (16)$$

where again total spin quantum number S' runs from zero to four inclusive, and each level has spin degeneracy $2S' + 1$ in the absence of an external field.

Calculation of Powder Susceptibility

Isolated Orbital Singlet Ground State. The susceptibility equation corresponding to the levels (eq 12) is obtained by a well-known procedure which leads to the formula

$$\chi_A' = \frac{1}{2}Ng^2\mu_B^2F(J,T)[kT - 2Z'J'F(J,T)]^{-1} + N\alpha \quad (17)$$

where

$$F(J,T) = 2$$

$$\times \left[\frac{14 + 30e^{8J/kT} + 5e^{-6J/kT} + e^{-10J/kT}}{7 + 9e^{8J/kT} + 5e^{-6J/kT} + 3e^{-10J/kT} + e^{-12J/kT}} \right] \quad (18)$$

In deriving eq 17 we have allowed for intercluster interaction in the molecular field approximation, as described by Ginsberg and Lines.¹¹ J' is the effective interdimer exchange integral, and Z' is the dimer lattice coordination number. $N\alpha$ is a correction term for the temperature independent paramagnetism.

Orbitally Dependent Exchange. In the presence of an applied magnetic field the levels (eq 16) split. The perturbation Hamiltonian is $-\mu_B(\mathbf{L}_1 + 2\mathbf{S}_1 + \mathbf{L}_2 + 2\mathbf{S}_2) \cdot \mathbf{H}$ where μ_B is the Bohr magneton and \mathbf{H} is the applied field. In first order, since there are no diagonal nonzero matrix elements of orbital angular momentum involved, this simplifies to $-g\mu_B\mathbf{S}' \cdot \mathbf{H}$ with $g = 2$. Since in reality the spin-orbit coupling energy will slightly mix the orbitals we shall treat the g factor as a parameter to be determined from experiment but shall ignore any anisotropy of the spin-orbitally induced increment $g - 2$ in the powder context and anticipate that $(g - 2)/2 \ll 1$. We do not calculate $(g - 2)/2$ within our model because admixtures from the higher levels $|0\rangle$ and ψ_{\pm} may well not be negligible in this context.

For an applied field in the z direction of Figure 2 the nonzero off-diagonal matrix elements of L_z from eq 11 allow for a nonzero quadratic (i.e., second order) perturbation from the field Hamiltonian $-\mu_B(L_1^2 + 2S_1^2 + L_2^2 + 2S_2^2)H_z$. For this case, using simple nondegenerate perturbation theory to second order, we find perturbed energies

$$\begin{aligned} E(+ + S'M) &= E_{++} - g\mu_B M H_z \\ &\quad + 2g^2\mu_B^2 H_z^2 A^2 (E_{++} - E_{+-})^{-1} \\ E(+ - S'M) &= E_{+-} - g\mu_B M H_z \\ &\quad + g^2\mu_B^2 H_z^2 A^2 [(E_{+-} - E_{++})^{-1} + (E_{+-} - E_{--})^{-1}] \\ E(- - S'M) &= E_{--} - g\mu_B M H_z \\ &\quad + 2g^2\mu_B^2 H_z^2 A^2 (E_{--} - E_{+-})^{-1} \end{aligned} \quad (19)$$

where E_{++} , E_{+-} , E_{--} are the unperturbed states of eq 16, and $E(- + S'M)$ levels are exactly the same as $E(+ - S'M)$. In general, therefore, the perturbed eigenlevels take the form

$$E_i = W_i + W_i' H_z + W_i'' H_z^2 \quad (20)$$

The calculation of the z -component susceptibility per dimer, χ_z^{dim} , from levels of this nature is straightforward¹² and takes the form

$$\chi_z^{\text{dim}} = \frac{\sum_i [(W_i'/kT) - 2W_i''] \exp(-W_i/kT)}{\sum_i \exp(-W_i/kT)} \quad (21)$$

where the sum over i includes, in our case, all one hundred levels $M = -S', \dots, +S'$; $S' = 0, 1, 2, 3, 4$; and the four orbital possibilities $++$, $+-$, $-+$, and $--$. The x and y component susceptibilities will differ from χ_z only in the absence of the W_i'' contributions.

The summation over M is easily performed analytically to obtain a final form

$$\begin{aligned} \chi_z^{\text{dim}}/g^2\mu_B^2 &= \sum_{S'} [(C - 2V_1)e^{-E_{++}/kT} \\ &\quad + (C - 2V_2)e^{-E_{+-}/kT} + 2(C - V_3 - V_4)e^{-E_{+-}/kT}] / \\ &\quad \sum_{S'} (2S' + 1)(e^{-E_{++}/kT} + e^{-E_{+-}/kT} + 2e^{-E_{+-}/kT}) \end{aligned} \quad (22)$$

where $S' = 0, 1, 2, 3, 4$ and

$$C = S'(S' + 1)(2S' + 1)/3kT \quad (23)$$

$$V_1 = 2A^2(2S' + 1)(E_{++} - E_{+-})^{-1} \quad (24)$$

$$V_2 = 2A^2(2S' + 1)(E_{--} - E_{+-})^{-1} \quad (25)$$

$$V_3 = 2A^2(2S' + 1)(E_{+-} - E_{++})^{-1} \quad (26)$$

$$V_4 = 2A^2(2S' + 1)(E_{+-} - E_{--})^{-1} \quad (27)$$

As mentioned above, the "transverse" susceptibility components have no Van Vleck contributions and are therefore obtained from eq 22 by setting $V_i = 0$ ($i = 1, 2, 3, 4$). The powder susceptibility per gram-atom of iron χ_A' is then obtained from the formula

$$\chi_A' = \frac{1}{3}(\chi_x^{\text{dim}} + \chi_y^{\text{dim}} + \chi_z^{\text{dim}}) \quad (28)$$

The powder susceptibility is therefore a function of six parameters namely the g -factor, crystal field splitting Δ , exchanges J_{++} , J_{+-} , J_{--} , and (via A) the mixing parameter γ (or more precisely γ^2).

Analysis of the Exchange Coupling

The exchange parameters J in the isolated orbital singlet model and J_{++} , J_{+-} , and J_{--} in the orbitally dependent exchange model are each the resultant of several electron-pair exchanges. We now analyze these parameters into component electron-pair exchange integrals between d orbitals oriented with their lobes along iron-sulfur bridge bonds or along the Fe...Fe internuclear direction. We will find that J_{++} , J_{+-} , and J_{--} may each be expressed in terms of the same three electron-pair exchanges. Through examination of the elementary d orbital overlaps a number of restrictions may be placed on the values of the pair exchange integrals. This makes the comparison of the model with experiment more stringent and leads to a description of exchange in $(\text{FeL}')_2$ and $(\text{FeL})_2$ in terms of "best fit" parameter values with physically understandable trends from one dimer to the other.

Appropriate metal centered coordinate systems for analysis of the exchange are labeled x_1' , y_1' , z_1' and x_2' , y_2' , z_2' in Figure 2. In these coordinate systems the d orbitals have their lobes along iron-sulfur bridge bonds or along the Fe...Fe internuclear distance or at 90° or 45° angles to these directions. Carrying out the required 30° coordinate rotation about the z -axis transforms the orbitals $\varphi_{\pm}^{(i)}$, $\psi_{\pm}^{(i)}$, and $d_{z^2}^{(i)}$ into

$$\begin{aligned} \varphi_+^{(i)} &= \eta(0.866d_{y_2 z_2'}^{(i)} + 0.5d_{x_2 z_2'}^{(i)} \\ &\quad + 0.5\gamma a_i d_{x_1 y_1'}^{(i)} + 0.433\gamma a_i d_{x_2 y_2'}^{(i)}) \\ \varphi_-^{(i)} &= \eta(0.866d_{x_2 z_2'}^{(i)} - 0.5d_{y_2 z_2'}^{(i)} \\ &\quad - 0.5\gamma a_i d_{x_2 y_2'}^{(i)} + 1.732\gamma a_i d_{x_1 y_1'}^{(i)}) \\ \psi_+^{(i)} &= \eta(0.5d_{x_2 y_2'}^{(i)} - 1.732d_{x_1 y_1'}^{(i)} \\ &\quad + 0.866\gamma a_i d_{x_2 z_2'}^{(i)} - 0.5\gamma a_i d_{y_2 z_2'}^{(i)}) \\ \psi_-^{(i)} &= \eta(0.5d_{x_1 y_1'}^{(i)} + 0.433d_{x_2 y_2'}^{(i)} \\ &\quad - 0.866\gamma a_i d_{y_2 z_2'}^{(i)} - 0.5\gamma a_i d_{x_2 z_2'}^{(i)}) \\ d_{z^2}^{(i)} &= d_{z^2}^{(i)} \end{aligned} \quad (29)$$

Table II. Exchange Coupling Pathways in (FeL')₂ and (FeL)₂

Overlap ^a type	Pathway ^b	Pair exchange parameter to which pathway contributes	Coupling contributes
direct σ	$d_{y'z'}(1) \parallel d_{y'z'}(2)$	Antiparallel	J_D
$\pi-\sigma$	$d_{y'z'}(1,2) \parallel p_z \parallel d_{z'2}(2,1)$	Antiparallel	$J_{\pi\sigma}$
$\pi-\sigma$	$d_{y'z'}(1,2) \parallel p_y \parallel d_{x'2} - y'2(2,1)$	Antiparallel	$J'_{\pi\sigma}$
$\pi-\sigma$	$d_{x'z'}(1,2) \parallel p_x \perp p_y \parallel d_{x'2} - y'2(2,1)$	Parallel	$J'_{\pi\sigma}$
$\pi-\sigma$	$d_{x'y'}(1,2) \parallel p_x \perp p_z \parallel d_{z'2}(2,1)$	Parallel	$J'_{\pi\sigma}$
$\sigma-\sigma$	$d_{z'2}(1,2) \parallel p_z \perp p_y \parallel d_{x'2} - y'2(2,1)$	Parallel	$J_{\sigma\sigma}$
$\sigma-\sigma$	$d_{z'2}(1,2) \parallel s \parallel d_{x'2} - y'2(2,1)$	Antiparallel	$J_{\sigma\sigma}$
$\sigma-\sigma^c$	$d_{z'2}(1,2) \parallel p_z \parallel d_{x'2} - y'2(2,1)$	Antiparallel	$J_{\sigma\sigma}$
$\sigma-\sigma^c$	$d_{z'2}(1,2) \parallel p_y \parallel d_{x'2} - y'2(2,1)$	Antiparallel	$J_{\sigma\sigma}$

^aPathways to which *only* π -overlap contributes are neglected.

^bNotation of ref 7: \parallel and \perp stand, respectively, for overlap and orthogonal. ^cThis pathway exists only when the Fe-S-Fe bridge angle deviates from 90°.

where $i = 1, 2$; $a_1 = +1$, $a_2 = -1$. Table II lists the significant exchange coupling pathways between d orbitals $d_{x'y'}^{(i)}$, $d_{x'z'}^{(i)}$, $d_{y'z'}^{(i)}$, $d_{x'2-y'2}^{(i)}$, and $d_{z'2}^{(i)}$, as arrived at by qualitative assessment of possible overlaps. Pathways involving only π -overlaps have been neglected. Examination of Table II shows that coupling between the d orbitals may be described in terms of four electron-pair exchange parameters. J_D is the parameter for coupling between electrons in $d_{y'z'}^{(1)}$ and $d_{y'z'}^{(2)}$ by direct overlap. Formally, we define J_D by the isotropic Hamiltonian $-2J_D \mathbf{S}_1 \cdot \mathbf{S}_2$, which represents the contribution of direct $y'z'-y'z'$ overlap to the total spin-two exchange. In an exactly analogous manner we define the other pair exchange parameters in Table II: $J_{\pi\sigma}$ for the exchange between $d_{y'z'}^{(1,2)}$ and $d_{z'2}^{(2,1)}$ or the equivalent exchange between $d_{y'z'}^{(1,2)}$ and $d_{x'2-y'2}^{(2,1)}$, $J'_{\pi\sigma}$ for the exchange between $d_{x'z'}^{(1,2)}$ and $d_{x'2-y'2}^{(2,1)}$ or the equivalent exchange between $d_{x'y'}^{(1,2)}$ and $d_{z'2}^{(2,1)}$, and $J_{\sigma\sigma}$ for the exchange between $d_{z'2}^{(1,2)}$ and $d_{x'2-y'2}^{(2,1)}$. The last two pathways in Table II occur only when the angle at the bridging sulfur deviates from 90° so that $d_{z'2}$ and $d_{x'2-y'2}$ are not orthogonal to, respectively, sulfur p_y and p_z orbitals.

Physically the direct exchange J_D is dominantly of kinetic origin¹³ and must be antiferromagnetic (i.e., negative) with a value extremely sensitive to the iron-iron distance. The exchange $J_{\pi\sigma}$ is also of dominantly kinetic origin and therefore negative; its magnitude will be a sensitive function of the Fe-S-Fe bridge angle being greatest for the right angle limit. If the bridge angle is truly a right angle $J_{\sigma\sigma}$ will be positive because of dominance of potential exchange via orthogonal ligand p orbitals over the kinetic contribution through the ligand s orbital. However, deviations of bridge angle from 90° introduce an antiferromagnetic kinetic component via nonorthogonal p orbitals which eventually changes the sign of this exchange. $J'_{\pi\sigma}$, like $J_{\sigma\sigma}$, will be positive for a 90° bridge angle but will tend toward negative as the angle deviates from 90° and antiferromagnetic kinetic terms compete with the potential exchange. In what follows we assume that $J'_{\pi\sigma} = J_{\sigma\sigma}$, since we expect both of these quantities to be small and of the same sign.

The relationship between J_{++} , J_{+-} , J_{--} and J_D , $J_{\pi\sigma}$, and $J_{\sigma\sigma}$ is now easy to establish. The exchange parameter J_{++} , for example, is relevant when the orbital dimer state is $|d^6, \varphi_{-}^{(1)}\rangle |d^6, \varphi_{-}^{(2)}\rangle$; the singly occupied orbitals on each ion are $d_{z'2}$, ψ_+ , ψ_- , and φ_+ . From eq A8 of the appendix we have

$$J_{++} = \sum_{i,j} J_{ij} \quad (30)$$

where the J_{ij} are exchange parameters for pair-wise interaction between the singly occupied orbitals, and the summation is over all 16 combinations of wave function pairs. A typical term in eq 30 is

$$J_{d_{z'2}^{(1)}\varphi_+^{(2)}} = \frac{1}{16} \{ \langle d_{z'2}^{(1)}(a)\varphi_+^{(2)}(b) | \mathcal{J}_{\text{ex}}^{\text{pot}} | d_{z'2}^{(1)}(b)\varphi_+^{(2)}(a) \rangle + \langle d_{z'2}^{(1)}(a) | \mathcal{J}_{\text{ex}}^{\text{kin}} | \varphi_+^{(2)}(a) \rangle^2 \} \quad (31)$$

where (a) and (b) label electrons and the operators are defined by eq A2 and A3 of the appendix. Substituting for φ_+ from eq 29 and expanding, eq 31 reduces to

$$J_{d_{z'2}^{(1)}\varphi_+^{(2)}} = \eta^2 [0.75J_{\pi\sigma} + 0.437\gamma^2 J_{\sigma\sigma}] \quad (32)$$

In a similar vein we have, for example, the $\psi_{-}^{(1)}-\psi_{-}^{(2)}$ contribution

$$J_{\psi_{-}^{(1)}\psi_{-}^{(2)}} = \frac{1}{16} \{ \langle \psi_{-}^{(1)}(a)\psi_{-}^{(2)}(b) | \mathcal{J}_{\text{ex}}^{\text{pot}} | \psi_{-}^{(1)}(b)\psi_{-}^{(2)}(a) \rangle + \langle \psi_{-}^{(1)}(a) | \mathcal{J}_{\text{ex}}^{\text{kin}} | \psi_{-}^{(2)}(a) \rangle^2 \} = \eta^4 \gamma^2 [0.75\gamma^2 J_D + 0.75J_{\pi\sigma} + 0.433J_{\sigma\sigma}] \quad (33)$$

Proceeding in this manner and summing all contributions for each case, ++, +-, -+, --, remembering the definition of η^2 as $(1 + \gamma^2)^{-1}$, we find

$$J_{++} = (1 - 0.5\eta^2 + 0.0624\eta^4)J_D + (2.375 - 0.094\eta^2 - 0.125\eta^4)J_{\pi\sigma} + (1.25 + 6.719\eta^2 - 0.375\eta^4)J_{\sigma\sigma} \quad (34)$$

$$J_{--} = (1 - 1.5\eta^2 + 0.562\eta^4)J_D + (2.5 - 1.5\eta^2 - 0.281\eta^4)J_{\pi\sigma} + (7 + 1.125\eta^2 - 0.0938\eta^4)J_{\sigma\sigma} \quad (35)$$

$$J_{+-} = J_{-+} = (1 - \eta^2 + 0.188\eta^4)J_D + (2.438 - 0.766\eta^2 - 0.234\eta^4)J_{\pi\sigma} + (4.125 + 3.891\eta^2 - 0.203\eta^4)J_{\sigma\sigma} \quad (36)$$

Substituting into eq 22 and 28 via the energies E_{++} , E_{+-} , and E_{--} of eq 16, the powder susceptibility for the orbitally dependent exchange model can now be computed directly in terms of the parameters γ and Δ and the physically recognized J_D , $J_{\pi\sigma}$, and $J_{\sigma\sigma}$.

Comparison of Theory and Experiment

Before comparing theory and experiment we observe that the g factor may be fixed by extrapolation to infinite temperature, in which limit the other parameters make no contribution: The relation

$$\mu_{\text{eff}}^2 = g^2 S(S+1) + \frac{g^2 S(S+1)\theta}{T} \quad (37)$$

where S is the total single-ion spin and θ is a Weiss constant, holds for small θ/T . Plots of μ_{eff}^2 against $1/T$ for both (FeL')₂ and (FeL)₂ are linear at high temperatures; we find $g(\text{FeL}')_2 = 2.15$ (from nine data points, 290–366 K), and $g(\text{FeL})_2 = 2.16$ (from ten data points, 324–372 K).

Isolated Orbital Singlet Ground State. This model, eq 17, has three variable parameters, namely J , $N\alpha$, and $Z'J'$. Since the crystal structures of (FeL')₂ and (FeL)₂ are built of isolated dimer molecules with minimum interdimer Fe...Fe separations exceeding 7 Å, the intercluster interaction $|Z'J'|$ must be small compared to $|J|$, and so long as J is negative $Z'J'$ will be negligible in its effect on the powder susceptibility even at very low temperatures.¹⁰ In comparing eq 17 with the data we therefore set $Z'J' = 0$ and varied only J and $N\alpha$. Figures 4 and 5 show the best fits obtained by means of a nonlinear least-squares fitting routine.¹⁴ It is evident that the isolated orbital singlet model fails completely to account for the observed temperature dependence of the susceptibility of (FeL')₂ and

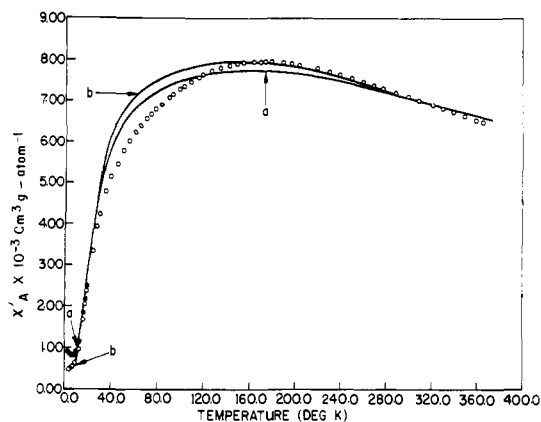


Figure 4. Nonlinear least-squares comparison of the isolated orbital singlet model (eq 17) with the $(\text{FeL}')_2$ susceptibility measurements; $g = 2.15$ and $Z'J' = 0$ were fixed. Experimental values corrected for the presence of paramagnetic impurity (see "Results" section) are shown as open circles, filled circles indicate the uncorrected values where the correction is significant. (a) Best fit to the entire data set: $J = -26 \text{ cm}^{-1}$, $N\alpha = 775 \times 10^{-6} \text{ cm}^3 \text{ g-atom}^{-1}$. (b) Best fit to the points above 120 K: $J = -24.5 \text{ cm}^{-1}$, $N\alpha = 540 \times 10^{-6} \text{ cm}^3 \text{ g-atom}^{-1}$.

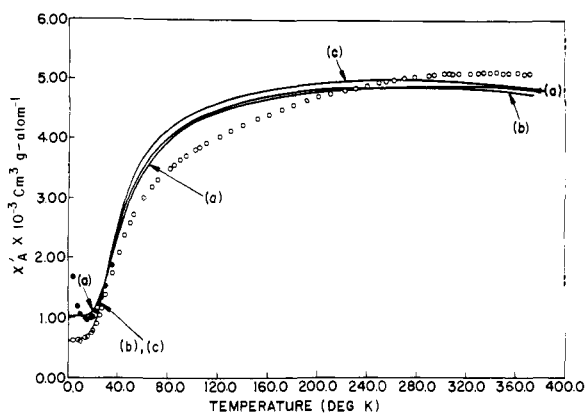


Figure 5. As Figure 4 but for the complex $(\text{FeL})_2$. $g = 2.16$, $Z'J' = 0$. (a) Best fit to the entire data set: $J = -47 \text{ cm}^{-1}$, $N\alpha = 1015 \times 10^{-6} \text{ cm}^3 \text{ g-atom}^{-1}$. (b) Best fit to the entire data set with fixed $N\alpha = 615 \times 10^{-6} \text{ cm}^3 \text{ g-atom}^{-1}$, the observed value at low temperatures: $J = -43 \text{ cm}^{-1}$. (c) Same as (b) except the fit is only to the points above 120 K: $J = -42 \text{ cm}^{-1}$.

$(\text{FeL})_2$. Even fits to the limited subset of data above 120 K show major deviations. Physically acceptable values of $Z'J'$ or the axial anisotropy parameter D ($|D| \lesssim 13 \text{ cm}^{-1}$) cannot explain the observed deviations.

Orbitally Dependent Exchange. With g fixed, this model has five variable parameters, namely γ , Δ , J_D , $J_{\pi\sigma}$, and $J_{\sigma\sigma}$. As discussed earlier there are a number of physical restrictions on the values which the parameters may assume; in summary they are

$$0 < \gamma < 1 \quad (38)$$

$$\gamma(\text{FeL}')_2 \approx \gamma(\text{FeL})_2 \quad (39)$$

$$0 < |\Delta| \lesssim 500 \text{ cm}^{-1} \quad (40)$$

$$J_D \leq 0 \quad (41)$$

$$J_{\pi\sigma} \leq 0 \quad (42)$$

$$|J_D(\text{FeL})_2| > |J_D(\text{FeL}')_2| \quad (43)$$

$$J_{\sigma\sigma} \text{ small + or -} \quad (44)$$

$$J_{\sigma\sigma}(\text{FeL}')_2 \geq J_{\sigma\sigma}(\text{FeL})_2 \quad (45)$$

$$|J_{\pi\sigma}(\text{FeL}')_2| \gtrsim |J_{\pi\sigma}(\text{FeL})_2| \quad (46)$$

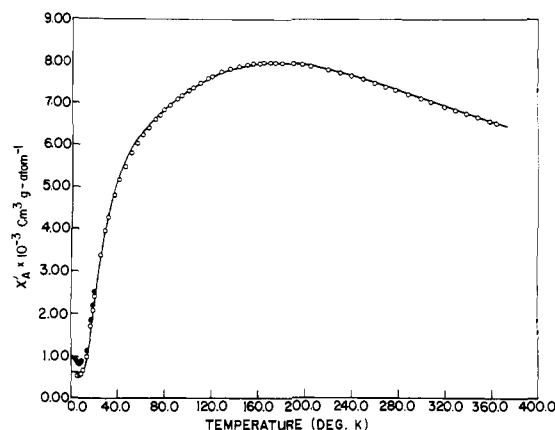


Figure 6. Least-squares best fit of orbitally dependent exchange model (eq 28) to the $(\text{FeL}')_2$ susceptibility data. See Table III for parameter values. Open and filled circles are, respectively, the experimental points with and without paramagnetic impurity correction (see "Results" section). Uncorrected points are shown only where they are significantly different from the corrected values.

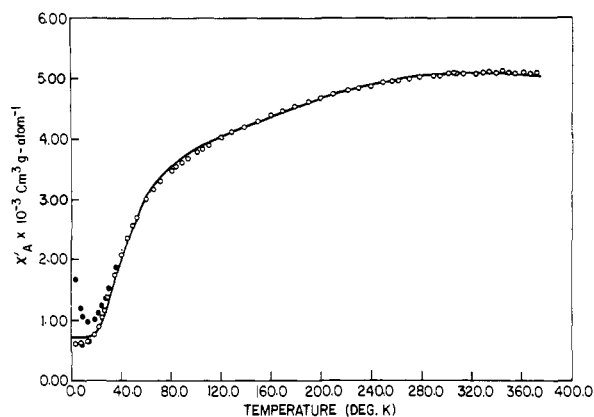


Figure 7. As Figure 6 but for the complex $(\text{FeL})_2$.

Table III. Best Fit Values of the Parameters for the Orbitally Dependent Exchange Model^a

Parameter ^b	$(\text{FeL}')_2$	$(\text{FeL})_2$
γ	0.52	0.36
Δ (cm^{-1})	$-102 \lesssim \Delta \lesssim -93$	$-235 \lesssim \Delta \lesssim -231$
J_D (cm^{-1}) ^c	$-22 \lesssim J_D \lesssim 0$	$-66 \lesssim J_D \lesssim -45$
$J_{\pi\sigma}$ (cm^{-1}) ^c	$-2 \gtrsim J_{\pi\sigma} \gtrsim -12$	$0 \gtrsim J_{\pi\sigma} \gtrsim -10$
$J_{\sigma\sigma}$ (cm^{-1}) ^c	$-1.3 \lesssim J_{\sigma\sigma} \lesssim 0$	$-1.3 \lesssim J_{\sigma\sigma} \lesssim 0$

^a Allowed values of the parameters constrained by relations eq 39, 41, 42, and 45. ^b $g(\text{FeL}')_2 = 2.15$ and $g(\text{FeL})_2 = 2.16$ were fixed. ^c The best fit values of J_D , $J_{\pi\sigma}$, and $J_{\sigma\sigma}$ fall within the ranges shown, but are not independent, being related by eq 47, 48 for $(\text{FeL}')_2$ and 49, 50 for $(\text{FeL})_2$. See discussion in text.

In carrying out the nonlinear least-squares comparison of eq 28 with the $(\text{FeL}')_2$ and $(\text{FeL})_2$ susceptibility data, we found that with J_D and $J_{\pi\sigma}$ restricted according to eq 41 and 42, equally good fits can be obtained for $\gamma \sim 0.5$ or 0.95 . However if, in addition, we invoke the restrictions eq 39 and 45 then only $\gamma \sim 0.5$ is consistent with the measurements. Figures 6 and 7 show the fits obtained under these conditions; the least-squares values of the parameters are summarized in Table III. Within the ranges given in the table the best fit values of J_D , $J_{\pi\sigma}$, and $J_{\sigma\sigma}$ are related as follows: For $(\text{FeL}')_2$,

$$J_{++} = 0.645J_D + 2.224J_{\pi\sigma} + 6.306J_{\sigma\sigma} = -27 \text{ cm}^{-1} \quad (47)$$

$$J_D + J_{\pi\sigma} - 9.26J_{\sigma\sigma} = -12.2 \text{ cm}^{-1} \quad (48)$$

For $(\text{FeL})_2$,

$$J_{++} = 0.606J_D + 2.194J_{\pi\sigma} + 6.904J_{\sigma\sigma} = -49.0 \text{ cm}^{-1} \quad (49)$$

$$J_D + J_{\pi\sigma} - 8.67J_{\sigma\sigma} = -54.6 \text{ cm}^{-1} \quad (50)$$

The existence of relations 47, 48 and 49, 50 means that for a given value of any one of the three exchange parameters within its range, the other two parameter values that give a least-squares best fit are determined by the applicable pair of relations. With this restriction any set of exchange parameter values within the ranges shown in Table III will give an equivalent fit to the data.

Equation 28, with the parameter values in Table III, is in excellent agreement with the experimental susceptibility vs. temperature curves for both $(\text{FeL}')_2$ and $(\text{FeL})_2$. Furthermore, the parameter values in Table III satisfy all nine constraints, eq 38–46. Taken together with the failure of the isolated orbital singlet model to account for the measurements, we regard this as good evidence that the exchange in $(\text{FeL}')_2$ and $(\text{FeL})_2$ is orbitally dependent in the sense defined in the introduction.

The orbitally dependent exchange theory provides an interesting description of exchange coupling in $(\text{FeL}')_2$ and $(\text{FeL})_2$. According to our analysis the antiferromagnetic coupling in $(\text{FeL})_2$, $d(\text{Fe}\cdots\text{Fe}) = 3.21 \text{ \AA}$, takes place predominantly by direct overlap of the $d_{y'z'}$ orbitals. Thus the lower limit on $|J_D|$ is 45 cm^{-1} and corresponds to an upper limit on $|J_{\pi\sigma}|$ of 10 cm^{-1} and an upper limit on $J_{\sigma\sigma}$ of 0 cm^{-1} . Apparently the potential and kinetic contributions to $J_{\sigma\sigma}$ cancel. For $(\text{FeL}')_2$, $d(\text{Fe}\cdots\text{Fe}) = 3.37 \text{ \AA}$, we find an upper limit on $|J_D|$ of 22 cm^{-1} ; the 0.16 \AA increase in iron–iron distance has caused a decrease in $|J_D|$ of at least 23 cm^{-1} or $\sim 50\%$. Overlap of the J_D and $J_{\pi\sigma}$ ranges for $(\text{FeL}')_2$ prevents any decision as to which makes the dominant contribution to the exchange coupling in this compound.

It is worth while to examine the values of J_{++} , J_{+-} , and J_{--} corresponding to the best fit values of J_D , $J_{\pi\sigma}$, and $J_{\sigma\sigma}$. We have already seen that $J_{++}(\text{FeL}')_2 = -27 \text{ cm}^{-1}$ and $J_{++}(\text{FeL})_2 = -49.0 \text{ cm}^{-1}$ are conditions relating the best fit values of the pair exchange parameters. Since Δ is negative the orbital dimer ground state is $|d^6, \varphi_{-}^{(1)}\rangle |d^6, \varphi_{-}^{(2)}\rangle$, and J_{++} is therefore the exchange coupling parameter for the molecular ground state. The ranges of J_{--} and J_{+-} may be calculated from eq 35 and 36. We find for $(\text{FeL}')_2$, $-21 \lesssim J_{+-} \lesssim -20 \text{ cm}^{-1}$, $-16 \lesssim J_{--} \lesssim -14 \text{ cm}^{-1}$, and for $(\text{FeL})_2$, $J_{+-} \approx -27 \text{ cm}^{-1}$, $-18 \lesssim J_{--} \lesssim -15 \text{ cm}^{-1}$. It is clear from these numbers that in the state $|d^6, \varphi_{-}^{(1)}\rangle |d^6, \varphi_{-}^{(2)}\rangle$, $(\text{FeL}')_2$ and $(\text{FeL})_2$ differ considerably in the strength of exchange coupling. The difference is much less in states $|d^6, \varphi_{-}^{(1)}\rangle |d^6, \varphi_{+}^{(2)}\rangle$ and $|d^6, \varphi_{+}^{(1)}\rangle |d^6, \varphi_{-}^{(2)}\rangle$, and still less in the state $|d^6, \varphi_{+}^{(1)}\rangle |d^6, \varphi_{+}^{(2)}\rangle$. This trend may be traced to the fact that orbital $\varphi_{+}^{(i)}$ has a larger $d_{y'z'}$ component than orbital $\varphi_{-}^{(i)}$. As a consequence the shorter $\text{Fe}\cdots\text{Fe}$ distance in $(\text{FeL})_2$ has its greatest effect in the state $|d^6, \varphi_{-}^{(1)}\rangle |d^6, \varphi_{-}^{(2)}\rangle$ and its smallest effect in the state $|d^6, \varphi_{+}^{(1)}\rangle |d^6, \varphi_{+}^{(2)}\rangle$.

The differences in the spin-level structures of $(\text{FeL}')_2$ and $(\text{FeL})_2$ may be seen from Figure 8. Both compounds have the $S' = 0, 1$, and 2 levels of $|d^6, \varphi_{-}^{(1)}\rangle |d^6, \varphi_{-}^{(2)}\rangle$ lowest in energy. However, they differ in that the splitting of these levels to low energy is much greater in $(\text{FeL})_2$ than in $(\text{FeL}')_2$. Also, the overall width of the spin manifold is much greater for the former than the latter compound (cf. 1178 cm^{-1} for $(\text{FeL})_2$ and 648 cm^{-1} for $(\text{FeL}')_2$). This is a consequence of the larger value of $|J_{++}|$, abetted by the larger $|\Delta|$, for $(\text{FeL})_2$. Above the $S' = 2$ level of $|d^6, \varphi_{-}^{(1)}\rangle |d^6, \varphi_{-}^{(2)}\rangle$, spin levels derived from $|d^6, \varphi_{+}^{(1)}\rangle |d^6, \varphi_{-}^{(2)}\rangle$, $|d^6, \varphi_{-}^{(1)}\rangle |d^6, \varphi_{+}^{(2)}\rangle$, and $|d^6, \varphi_{+}^{(1)}\rangle |d^6, \varphi_{+}^{(2)}\rangle$ appear below levels derived from the ground orbital state.

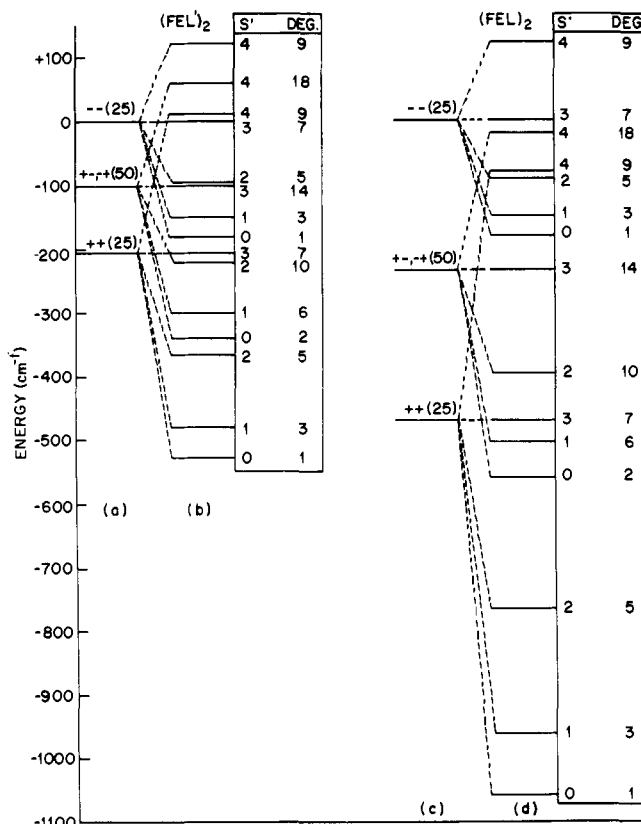


Figure 8. Spin energy level diagrams for $(\text{FeL}')_2$ and $(\text{FeL})_2$. (a) and (c) show the four lowest dimer orbital states in the absence of exchange; ++, +-, -+, and -- refer, respectively, to $|d^6, \varphi_{-}^{(1)}\rangle |d^6, \varphi_{-}^{(2)}\rangle$, $|d^6, \varphi_{-}^{(1)}\rangle |d^6, \varphi_{+}^{(2)}\rangle$, $|d^6, \varphi_{+}^{(1)}\rangle |d^6, \varphi_{-}^{(2)}\rangle$, and $|d^6, \varphi_{+}^{(1)}\rangle |d^6, \varphi_{+}^{(2)}\rangle$. The numbers in parentheses give the total degeneracy of the state. (b) and (d) show the exchange splitting of the dimer states; the total spin S' and remaining degeneracy are given to the right of each level. Parameter values (cm^{-1}) used in constructing the diagrams are: $\Delta = -102$, $J_{++} = -27$, $J_{+-} = J_{-+} = -20$, $J_{--} = -15$ for $(\text{FeL}')_2$ and $\Delta = -235$, $J_{++} = -49$, $J_{+-} = J_{-+} = -27$, $J_{--} = -15$ for $(\text{FeL})_2$.

We may now summarize the principal new results reported in this paper: (1) The notion of orbitally dependent exchange is defined, and a theory based on this idea is shown to account quantitatively, in a physically understandable manner, for the susceptibility vs. temperature curves of the complexes $(\text{FeL}')_2$ and $(\text{FeL})_2$. (2) Because the exchange in $(\text{FeL}')_2$ and $(\text{FeL})_2$ is orbitally dependent it is possible to evaluate the electron pair exchange parameters, contributing to the net exchange between iron atoms, from the temperature dependence of the susceptibility. Evaluation of pair exchange parameters from susceptibility vs. temperature data should be possible in general when orbitally dependent exchange occurs; it is not possible for isolated orbital singlet exchange, except, of course, when only a single pair parameter contributes to the exchange. (3) Two Fe^{2+} atoms 3.21 \AA apart can engage in significant antiferromagnetic exchange ($|J_D| \sim 50 \text{ cm}^{-1}$) by direct overlap of $3d$ -orbitals pointed along the iron–iron internuclear line. This direct exchange is extremely sensitive to distance and an increase of 0.16 \AA in $d(\text{Fe}\cdots\text{Fe})$ causes a decrease of at least $\sim 50\%$ in the exchange parameter.

Finally, we note that a recent x-ray structure determination¹⁵ has revealed that bis(*N,N*-diethyldithiocarbamato)iron(II) has a structure very similar to $(\text{FeL})_2$: It is dimeric with two bridging sulfur atoms, distorted trigonal-bipyramidal coordination around each iron atom, and an $\text{Fe}\cdots\text{Fe}$ distance of 3.50 \AA . The temperature dependence ($295\text{--}89 \text{ K}$) of the magnetic susceptibility of the diethyldithiocarbamato complex, as well as other bis(*N,N*-dialkyldithiocarbamato)iron(II) complexes, appears not to be well described by the isotropic

spin-coupling Hamiltonian.¹⁶ We expect that the exchange coupling in these compounds will be found to be orbitally dependent. Measurements to liquid helium temperature are required to test this prediction.

Acknowledgment. This work was supported in part by Public Health Service Grant No. GM-16449 to S.J.L.

Appendix

The exchange operator for potential exchange between magnetic ions at sites *a* and *b* can most generally be expressed as¹⁷

$$\mathcal{H}_{\text{ex}} = \sum_{\sigma, \sigma'} \sum_{i, j, k, l} -\mathcal{J}_{ijkl} C_{b\sigma'}^\dagger C_{b\sigma} C_{a\sigma}^\dagger C_{a\sigma'} \quad (\text{A1})$$

in which *i, j, k, l* label magnetic orbitals, σ and σ' label spin eigenstates (with eigenvalues $\pm 1/2$), *C* and *C*[†] are, respectively, annihilation and creation operators for the orbitals, and

$$\mathcal{J}_{ijkl} = \mathcal{J}_{ijkl}^{\text{pot}} = +\frac{1}{2} \int \int \Phi_b^*{}^j(\mathbf{r}') \Phi_a^*{}^k(\mathbf{r}) \times \frac{e^2}{|\mathbf{r} - \mathbf{r}'|} \Phi_b^l(\mathbf{r}) \Phi_a^i(\mathbf{r}') d\mathbf{r} d\mathbf{r}' \quad (\text{A2})$$

In the most general form the eigenstates of the single ion problem are two component spin vectors with different and possibly complex orbital parts Φ . For kinetic exchange¹³ the form eq A1 is again appropriate but where now

$$\mathcal{J}_{ijkl} = \mathcal{J}_{ijkl}^{\text{kin}} = -U^{-1} \times \int \Phi_b^*{}^j(\mathbf{r}) h \Phi_a^i(\mathbf{r}) d\mathbf{r} \int \Phi_b^l(\mathbf{r}') h^* \Phi_a^*{}^k(\mathbf{r}') d\mathbf{r}' \quad (\text{A3})$$

in which *h* is the one-electron Hamiltonian of the crystal and *U* is an intraion repulsion energy.

Since both $\mathcal{J}_{ijkl}^{\text{pot}}$ and $\mathcal{J}_{ijkl}^{\text{kin}}$ are spin independent, one readily verifies that the only nonzero matrix elements of eq A1 are

$$\langle b, j, \pm 1/2; a, k, \pm 1/2 | \mathcal{H}_{\text{ex}} | b, l, \pm 1/2; a, i, \pm 1/2 \rangle = -\mathcal{J}_{ijkl}$$

and

$$\langle b, j, \pm 1/2; a, k, \mp 1/2 | \mathcal{H}_{\text{ex}} | b, l, \mp 1/2; a, i, \pm 1/2 \rangle = -\mathcal{J}_{ijkl}$$

and that therefore eq A1 can be reexpressed as

$$\mathcal{H}_{\text{ex}} = \sum_{i, j, k, l} -\mathcal{J}_{ijkl} C_b^\dagger C_b C_a^\dagger C_a (\frac{1}{2} + 2\mathbf{s}_a \cdot \mathbf{s}_b) \quad (\text{A4})$$

where \mathbf{s}_a and \mathbf{s}_b are spin half operators at sites *a* and *b*, respectively.

In any particular problem the form eq A4 can be expanded into components involving only real orbitals the contributions of which can be estimated (at least as to which terms are essential and which are negligible) by physical overlap arguments. For the case where the single ion eigenstates each take the form of a simple product of a single real orbital function and a two component spin vector the exchange form (eq A4) takes its simplest possible form

$$\mathcal{H}_{\text{ex}} = \sum_{i, j} -\mathcal{J}_{ij} (\frac{1}{2} + 2\mathbf{s}_a \cdot \mathbf{s}_b) \quad (\text{A5})$$

where $\mathcal{J}_{ij} \equiv \mathcal{J}_{ijij}$.

In this case, which is that appropriate for the present paper, the spin independent term in eq A5 can now be dropped for calculations involving thermodynamics, to give

$$\mathcal{H}_{\text{ex}} = \sum_{i, j} -2\mathcal{J}_{ij} \mathbf{s}_a \cdot \mathbf{s}_b \quad (\text{A6})$$

in which *i* and *j* run over all magnetic (i.e., singly occupied) orbitals, and where $\mathcal{J}_{ij} = \mathcal{J}_{ijij} = \mathcal{J}_{ijij}^{\text{pot}} + \mathcal{J}_{ijij}^{\text{kin}}$ can be calculated from eq A2 and A3. Hamiltonian (eq A6) is transformed to the total spin form by noting that the Hunds rule restriction constrains the magnetic electrons on the single-ions to have parallel spins. If the single-ion total spin is *S*, then within the $|S, M\rangle$ manifold

$$\begin{aligned} \mathbf{s}_a &= \frac{1}{2S} \mathbf{S}_a \\ \mathbf{s}_b &= \frac{1}{2S} \mathbf{S}_b \\ \mathbf{s}_a \cdot \mathbf{s}_b &= \frac{1}{4S^2} \mathbf{S}_a \cdot \mathbf{S}_b \end{aligned} \quad (\text{A7})$$

Making the conventional definition $J_{ij} = (1/4S^2)\mathcal{J}_{ij}$, we can write

$$\sum_{i, j} -2\mathcal{J}_{ij} \mathbf{s}_a \cdot \mathbf{s}_b = \sum_{i, j} -2J_{ij} \mathbf{S}_a \cdot \mathbf{S}_b = -2J_{ab} \mathbf{S}_a \cdot \mathbf{S}_b \quad (\text{A8})$$

References and Notes

- (1) Part 10: M. E. Lines, A. P. Ginsberg, and F. J. DiSalvo, *J. Chem. Phys.*, **61**, 2095 (1974).
- (2) (a) Bell Laboratories. (b) Columbia University.
- (3) W. J. Hu and S. J. Lippard, *J. Am. Chem. Soc.*, **96**, 2366 (1974).
- (4) K. Karlin and S. J. Lippard, *J. Am. Chem. Soc.*, preceding paper in this issue.
- (5) A. P. Ginsberg, R. L. Cohen, F. J. DiSalvo, and K. W. West, *J. Chem. Phys.*, **60**, 2657 (1974).
- (6) P. W. Selwood, "Magnetochemistry", 2d ed, Interscience, New York, N.Y., 1956, pp 78, 92.
- (7) (a) A. P. Ginsberg, *Inorg. Chim. Acta Rev.*, **5**, 45 (1971). (b) The final outcome of the subsequent calculations would be the same if we began by idealizing the dimer configuration to a regular square pyramid; the intermediate details would, of course, be different.
- (8) See, for example, H. Watanabe, "Operator Methods in Ligand Field Theory", Prentice-Hall, Englewood Cliffs, N.J., 1966.
- (9) M. E. Lines, A. P. Ginsberg, R. L. Martin, and R. C. Sherwood, *J. Chem. Phys.*, **57**, 1 (1972).
- (10) A. P. Ginsberg, R. L. Martin, R. W. Brookes, and R. C. Sherwood, *Inorg. Chem.*, **11**, 2884 (1972).
- (11) A. P. Ginsberg and M. E. Lines, *Inorg. Chem.*, **11**, 2289 (1972).
- (12) See, for example, J. H. Van Vleck, "The Theory of Electric and Magnetic Susceptibilities", Oxford University Press, London, 1932.
- (13) P. W. Anderson in "Magnetism", Vol. 1, G. T. Rado and H. Suhl, Ed., Academic Press, New York, N.Y., 1963, Chapter 2.
- (14) Bell Laboratories subroutine NLLSQ by W. A. Burnette and C. S. Roberts. This is an improved version of Share Program Library SDA 3094 by D. W. Marquardt.
- (15) O. A. Illeperuma and R. D. Feltham, *Inorg. Chem.*, **14**, 3042 (1975).
- (16) B. W. Fitzsimmons, S. E. Al-Mukhtar, L. F. Larkworthy, and R. R. Patel, *J. Chem. Soc., Dalton Trans.*, 1969 (1975).
- (17) F. Hartmann-Boutron, *J. Phys. (Paris)*, **29**, 212 (1968).